

Stoichiometry and mechanical properties of Mo_3Si

I. Rosales, J.H. Schneibel *

Metals and Ceramics Division, Oak Ridge National Laboratory, PO Box 2008, Oak Ridge, TN 37831-6115, USA

Received 18 September 1999; accepted 23 March 2000

Abstract

The A15 phase Mo_3Si is an important constituent of a new class of silicides based on Mo–Si–B. In this research it will be shown that, contrary to published results, single-phase Mo_3Si is slightly off-stoichiometric. In addition, it remains single phase in a small composition range. Its room temperature fracture toughness is on the order of $3 \text{ MPa m}^{1/2}$. The compressive strength at 1400°C in argon decreases with decreasing strain rate and increasing Si concentration. © 2000 Elsevier Science Ltd. All rights reserved.

Keywords: A. Molybdenum silicides; B. Fracture toughness; B. Yield stress

1. Introduction

Silicide intermetallics based on Mo, Si and B are currently of interest as potentially oxidation resistant, high temperature structural alloys [1–9]. One type consists of Mo_5SiB_2 , Mo_3Si , and a toughening α -Mo phase [5–9], another consists of Mo_3Si , Mo_5Si_3 , and Mo_5SiB_2 [1–4]. The phase Mo_5Si_3 has been studied in considerable detail. The elastic constants of Mo_5Si_3 determined by Fu et al. [10] by ab-initio calculations are in good agreement with Chu et al.'s experiments [11]. Meyer et al. [1] investigated the high temperature creep properties of powder metallurgical Mo_5Si_3 at compressive stresses of 120–180 MPa. Some research has also been performed for Mo_3Si . Fig. 1 shows a section of the Mo–Si binary phase diagram. Mo_3Si forms by a peritectic reaction at 2025°C . Christensen [12] prepared single crystals of Mo_3Si and investigated them by neutron scattering. Consistent with the phase diagram in Fig. 1, Christensen found Mo_3Si to be a line compound. Meyer et al. [1] found a high density of dislocations in the Mo_3Si phase in a three-phase Mo_5Si_3 – Mo_5SiB_2 – Mo_3Si alloy after creep testing at temperatures near 1300°C . The slip system was consistent with $(001) \langle 100 \rangle$. Misra et al. investigated the microstructure and mechanical properties of a Mo_3Si – Mo_5Si_3 eutectic composite [13]. Using an indentation cracking technique, they determined the room temperature fracture toughness to be 1 – $1.5 \text{ MPa m}^{1/2}$. Raj [14]

investigated the oxidation and mechanical properties of a ternary $(\text{Cr},\text{Mo})_3\text{Si}$ compound. Using a single-edge pre-cracked beam technique, he found room temperature fracture toughness values on the order of 2 – $3 \text{ MPa m}^{1/2}$. The purpose of the present work is to add to our knowledge of binary Mo_3Si . We will verify its single-phase composition, determine its room temperature fracture toughness and hardness, and assess its high temperature strength.

2. Experimental procedure

Alloys with nominal silicon concentrations ranging from 22 to 28 at.% were prepared by arc-melting of nominally pure elements in a partial pressure of argon (99.999% purity). Prior to melting, a Zr getter was melted to remove residual oxygen from the pumping chamber. The alloys were drop-cast into water-cooled copper molds with a diameter of 12.5 mm. Table 1 shows the nominal compositions and the compositions calculated by assuming that the weight loss during melting and casting were due to evaporation of either Si or Mo (since Si has a higher vapor pressure than Mo, it is assumed that the weight loss is due to loss of Si). A comparison with the nominal compositions shows that the actual Si concentrations of the cast specimens were lower than the nominal ones by typically 0.1–0.9 at.% (all discussions in this report will refer to nominal composition). Inductively coupled plasma (ICP) analysis by a commercial vendor resulted in substantially lower Si contents. As

*Corresponding author. Tel.: +1-865-576-4644; fax: +1-865-574-7659
E-mail address: schneibel@ornl.gov (J.H. Schneibel)

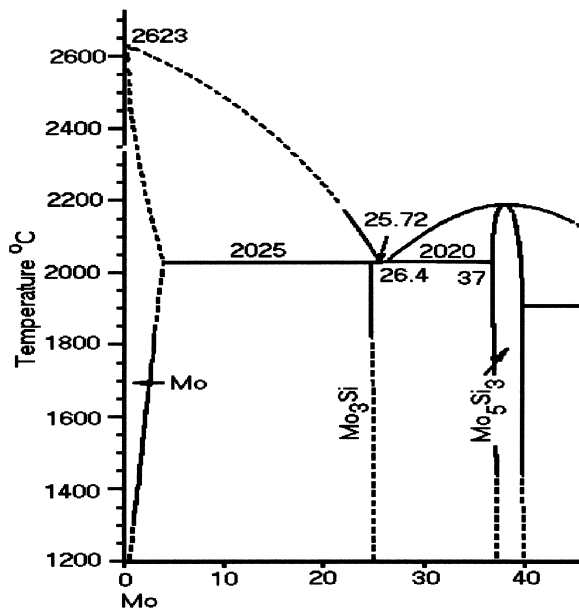


Fig. 1. A section of the binary Mo–Si phase diagram showing the compositions of the Mo_3Si and Mo_5Si_3 phases [14].

pointed out by Huebsch et al. [16], the calculations from the weight losses were the best option for determining the compositions. The specimens were annealed in a vacuum of 10^{-4} Pa for 24 h at 1600°C , and then cooled using a cooling rate of 2.5°C s^{-1} between 1600 and 1000°C . After metallographic polishing, the specimens were etched with Murakami's reagent for 1–2 s. The etched specimens were observed in an optical microscope as well as a scanning electron microscope equipped with an energy dispersive spectroscopy (EDS) system for determining the Mo:Si ratios in the alloys. The lattice parameters were determined by X-ray diffraction of powders with a size of $<45 \mu\text{m}$ and an internal silicon standard. The experimental accuracy of the lattice parameter measurements was estimated to be $3 \times 10^{-4} \text{ \AA}$. Pycnometric densities of coarse 40–80 mesh powder ground from the castings were determined in a He pycnometer. Microhardnesses were measured with a Buehler microhardness tester at a load of 500 g and a holding time of 15 s. Standard deviations were calculated from 10 measurements each. Fracture toughnesses were measured at room temperature using three-point flexure bars with

cross-sections of $3 \times 4 \text{ mm}$, a span of 10 mm, and an electro discharge machined single-edge notch with a depth of 2 mm. The fracture toughnesses were calculated from the maximum load according to the corresponding equation in ASTM standard E399-90 [17]. Compression specimens with dimensions of $2 \times 2 \times 4 \text{ mm}$ were also machined. They were compressed in an Instron 4501 testing machine at 1400°C in argon. In order to know the dependence of the yield stress on the strain rate, different initial strain rates of 10^{-3} , 1.8×10^{-4} and 10^{-5} s^{-1} were chosen.

3. Results and discussion

3.1. Microstructure

Fig. 2 shows optical micrographs of Mo_3Si specimens with different Si concentrations. As expected from the phase diagram, the specimen with 22 at.% Si contains $\alpha\text{-Mo}$ precipitates in a Mo_3Si matrix (Fig. 3a). These precipitates were identified by EDS as well as X-ray powder diffraction. They are at the grain boundaries suggesting that they controlled grain growth during the heat treatment. The specimen with 25 at.% Si (Fig. 2c) contains small particles of Mo_5Si_3 in a Mo_3Si matrix. Its grain size (not visible in Fig. 2c) was much larger than that of Mo–22 at.% Si. The specimen with 24 at.% Si (Fig. 2b) has also a large grain size because it does not contain second phases impeding its grain growth. Consistent with X-ray analysis, this alloy is single phase. Calculations of the single phase composition of “ Mo_3Si ” were also made based on the measured precipitate volume fractions in Mo–22 at.% Si and Mo–25 at.% Si. In both cases a single phase composition near 24 at.% Si was predicted from the overall compositions and the measured volume fractions of $\alpha\text{-Mo}$ or Mo_5Si_3 , respectively. In disagreement with the published Mo–Si phase diagram, the results of this study suggest that the single phase composition of Mo_3Si after cooling from 1600°C is not Mo–25 at.% Si, but near Mo–24 at.% Si.

3.2. Lattice parameter

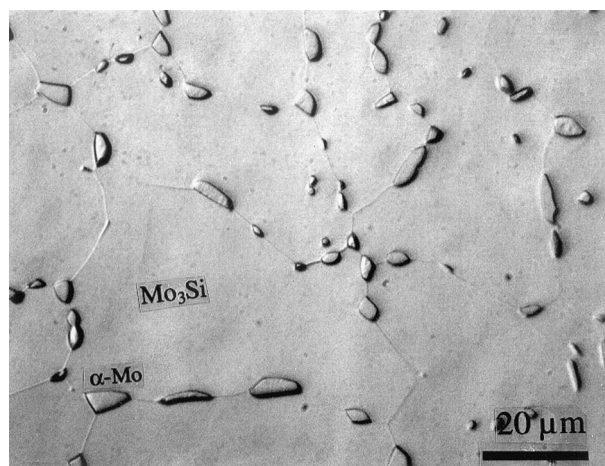
Fig. 3 shows the room temperature lattice parameter as a function of silicon concentration. If Mo_3Si were a true

Table 1

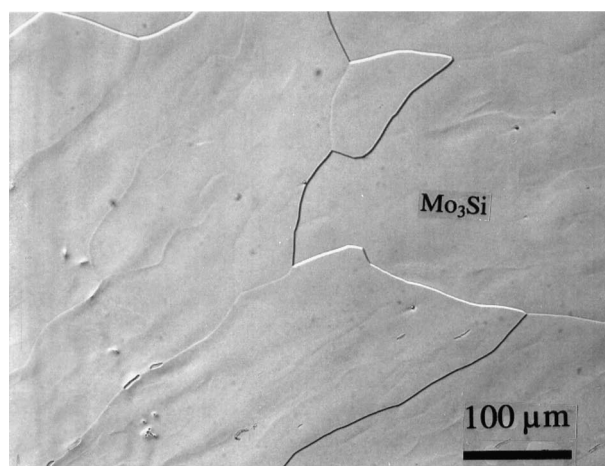
Nominal compositions of Mo_3Si and the compositions calculated by assuming the weight loss during melting and casting to be due either Si or Mo evaporation

Nominal Si concentration (at.%)	22.0	23.0	23.5	24.0	24.5	25.0	28.0
Initial mass of Si (g)	4.58	3.22	3.30	5.92	3.47	2.67	3.07
Initial mass of Mo (g)	55.42	36.78	36.70	64.08	36.53	27.33	26.93
Weight loss after melting (g)	0.25	0.068	0.105	0.04	0.036	0.06	0.002
Concentration of Si calculated from weight loss (at.% due to Si evaporation)	21.06	22.64	22.92	23.86	24.30	24.59	28.00
Concentration of Si calculated from weight loss (at.% due to Mo evaporation)	22.09	23.05	23.55	23.88	24.52	25.07	28.03

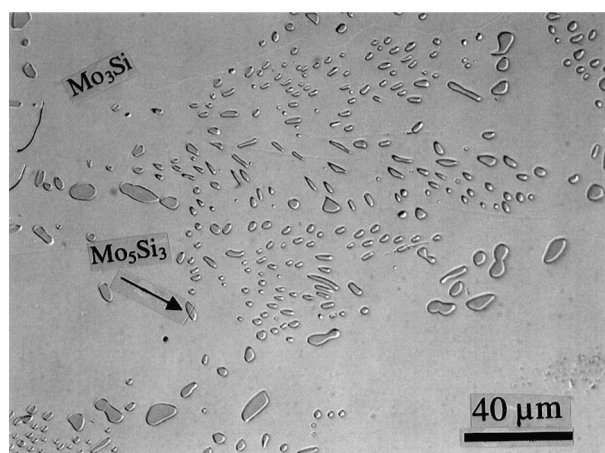
line compound, one would not expect a change in the lattice parameter as the Si concentration crosses the single phase composition. Fig. 3 shows, however, a lattice parameter change between 23.5 and 24 at.% Si. This



(a)



(b)



(c)

Fig. 2. Optical micrographs of etched specimens with (a) Mo–22 at.% Si with α -Mo precipitates; (b) single-phase Mo–24 at.% Si; (c) Mo–25 at.% Si with Mo_5Si_3 precipitates.

indicates a limited compositional range of the single phase, on the order of 0.5 at.% or less. Fig. 3 is consistent with the metallographic observation that the single phase composition is near 24 at.% Si.

Between 23.5 and 24 at.% Si, the lattice parameter in Fig. 3 decreases with a slope of $-0.007 \text{ \AA/at.\% Si}$. Since Si is a smaller atom than Mo, such a decrease is expected. A hard sphere model was used to estimate the change in lattice parameter with Si concentration. The Goldschmidt radii for Si and Mo (1.34 and 1.40 \AA , respectively [18]) were used, and adjacent Mo atoms in Mo_3Si were allowed to overlap. Substitution of the Si atoms by Mo resulted in a lattice parameter increase of 0.1 \AA , corresponding to a slope of $-0.004 \text{ \AA/at.\% Si}$. The similarity between the measured and predicted slopes shows that the slope in Fig. 3 is physically reasonable. Following Zhu et al. [19] the vacancy concentrations determined from X-ray and pycnometric densities were found to be on the order of 0.1 at.%. These values are on the order of the experimental error. This means that, for the heat treatment used in the current study, Mo_3Si contains less than 0.1 at.% thermal vacancies.

3.3. Microhardness

Table 2 shows the hardnesses of Mo_3Si alloys after furnace cooling from 1600°C or quenching from 1200°C

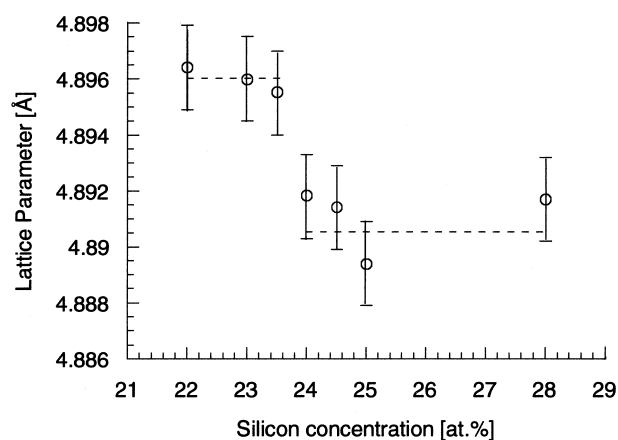


Fig. 3. Lattice parameters of cast and annealed (24 h/1600°C) Mo–Si alloys as a function of Si concentration.

Table 2

Microhardness of Mo–Si alloys for furnace cooled as well as quenched specimens

Silicon concentration (at.%)	Microhardness HVN (0.5) ^a	Microhardness HVN (0.5) ^b
22	1280±39	1295±43
24	1318±26	1322±22
25	1304±41	1322±35

^a Annealed 24 hr/1600°C/furnace cooled.

^b Annealed 2 hr/1200°C/oil quenched.

into oil. The indentations for these measurements were placed only in the matrix phase. In all cases, microcracks originated from the corners of the indent. Within the scatter of the measurements there was no distinct trend in the hardness as a function of Si concentration. Consistent with the absence of significant vacancy concentrations, the hardness of quenched Mo₃Si was similar to that of furnace cooled Mo₃Si.

3.4. Fracture toughness

Table 3 shows the fracture toughnesses of three Mo–Si alloys. For each alloy, two measurements were obtained. Since the Mo–22 at.% Si alloy contains α -Mo particles, some ductile phase toughening would be expected. However, the scatter in the measurements was too high to observe this trend. It should also be noted that the α -Mo volume fraction in Mo–22 at.% Si is small (see Fig. 3a). Quantitative metallography showed it to be only 8.0 vol.% and therefore not much toughening would be expected. The data in Table 3 indicate an average value on the order of 3.0 MPa m^{1/2}. The low value of one Mo–24 at.% Si specimen probably indicates the presence of a crack below the surface of the notch.

3.5. Compression tests

Fig. 4 shows the 0.2% offset yield stresses determined from compressive engineering stress–strain curves for Mo–22 at.% Si, Mo–24 at.% Si, and Mo–25 at.% Si deformed at 1400°C with initial strain rates of 10^{−3}, 1.8×10^{−4} and 10^{−5} s^{−1}, respectively (the stresses were

evaluated from the load and the initial cross sectional area of the specimens). As would be expected, the yield stress decreases with decreasing strain rate. Although Mo–22 at.% Si contains α -Mo precipitates, its yield stress is higher than that of Mo–24 at.% Si. This is somewhat unexpected since α -Mo at 1400°C has a yield strength of 83 MPa [20], which is lower than that of Mo₃Si (see Fig. 4 for 10^{−3}s^{−1}). One possible explanation for this finding is that the α -Mo particles may reduce internal cracking during compression. For high Si concentrations (25 at.%), Mo₅Si₃ precipitates form. Because of their high thermal expansion anisotropy [10], they may enhance internal cracking, and this may result in lower observed stress. Also, the defect populations in Mo₃Si may be different depending on whether the compound is Si-poor or rich, and this might give rise to different strengths.

4. Summary

We have shown that the A15 silicide Mo₃Si is not precisely stoichiometric, nor is it a true line compound. Its single phase composition is near Mo–24 at.% Si. After furnace cooling from 1600°C, the width of the single phase region is on the order of 0.5%. Within experimental accuracy (0.1 at%), furnace cooled Mo₃Si does not contain thermal vacancies. Its room temperature fracture toughness is on the order of 3.0 MPa m^{1/2}. Finally, the strength at 1400°C depends on the Si concentration and the strain rate.

Acknowledgements

This research was sponsored by the Division of Materials Sciences, US Department of Energy under contract number DE-AC05-00OR22725 with Oak Ridge National Laboratory, managed by UT-Battelle, LLC. The authors are grateful to C.A. Carmichael, J. Wright and E. Lee. Thanks go to J.A. Horton and C.G. McKamey of ORNL for reviewing this manuscript. I. Rosales acknowledges partial support by the Universidad Nacional Autonoma de México (UNAM-DGEP).

References

- [1] Meyer MK, Kramer MJ, Akinc M. Intermetallics 1996;4:273–81.
- [2] Meyer ML, Kramer MJ, Akinc M. Adv Mater 1996;8:85–8.
- [3] Schneibel JH, Liu CT, Heatherly L, Kramer MJ. Scr Mater 1998;38:1169–76.
- [4] Schneibel JH, Liu CT, Heatherly L, Kramer MJ. Scr Mater 1998;39:831.
- [5] Berczik DM. US patent no. 5,595,616, 21 January 1997.
- [6] Berczik DM. US patent no. 5,693,156, 2 December, 1997.
- [7] Nunes CA, Sakidja R, Perepezko JH. In: Nathal MV et al., editors. Structural intermetallics 1997, Warrendale, (PA): TMS, 1997. 831–9
- [8] Schneibel JH, Liu CT, Easton DS, Carmichael CA. Mater Sci Eng 1999;A26:78–83.

Table 3

Room temperature fracture toughnesses of Mo–Si alloys

at.% Si	22	24	25
K_Q (MPa m ^{1/2})	3.05	3.73	3.49
K_Q (MPa m ^{1/2})	3.39	2.09	2.9

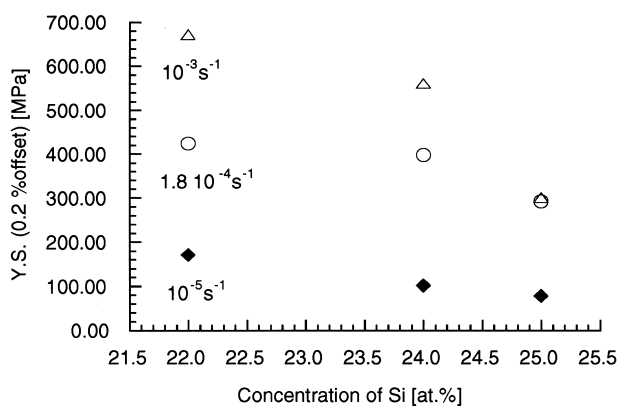


Fig. 4. Plot of 1400°C 0.2% offset yield strength vs. silicon concentration with initial strain rate of 10^{−3} s^{−1}, 1.8×10^{−4} s^{−1} and 10^{−5} s^{−1}.

- [9] Liu CT, Schneibel JH, Heatherly L. In: High-temperature ordered intermetallic alloys VII. MRS Symposium Proceedings, vol 552, 1999. p. KK6.2.1–7.
- [10] Fu CL, Xindong W, Ye YY, Ho KM. *Intermetallics* 1999;7:179–84.
- [11] Chu F, Thoma DJ, McClennan K, Peralta P, He Y. *Intermetallics* 1999;7:611–20.
- [12] Christensen NA. *Acta Chemica Scandinavica* 1983;A37:519–22.
- [13] Misra A, Petrovic JJ, Mitchell TE. *Scripta Mater* 1999;40:191–6.
- [14] Raj SV. *Mater Sci Eng* 1995;A201:229–41.
- [15] Gokhale AB, Baschian GJ. In: Binary alloys phase diagrams. Metals Park (OH): ASM, 1986. p. 1632.
- [16] Huebsch JH, Kramer MJ, Zhao HL, Akinc M. *Intermetallics* 2000;8:143–50.
- [17] Anon. Standard test method for plane-strain fracture toughness of metallic materials (E399-90). ASTM, 1990.
- [18] Laves F. Crystal struct. and atomic size. In: Theory of alloy phases. ASM, 1956 p. 131.
- [19] Zhu JH. *Acta Mater* 1999;47:2003–18.
- [20] Tietz TE, Wilson JW. Behavior and properties of refractory metals. Stanford (CA): Stanford University Press, 1965. p. 162.